Advancement in Sewage Sludge Dewatering with Hydrate Crystal Phase Change: Unveiling the Micro-Moisture Migration and Dewaterability Mechanisms

ACS Sustainable Chemistry & Engineering

pubs.acs.org/journal/ascecg

Research Article

Advancement in Sewage Sludge Dewatering with Hydrate Crystal Phase Change: Unveiling the Micro-Moisture Migration and Dewaterability Mechanisms

Lingjie Sun, Aliakbar Hassanpouryouzband, Huilian Sun, Tian Wang, Lunxiang Zhang,* Lei Yang, Jiafei Zhao,* and Yongchen Song

Cite This: *ACS Sustainable Chem. Eng.* 2023, 11, 12075−12083

Read Online

ACCESS | Metrics & More | Article Recommendations | Supporting Information

ABSTRACT: Sludge dewatering plays a crucial role in reducing the sludge volume, facilitating transportation, and enhancing energy recovery. However, conventional mechanical dewatering methods often generate high-concentration organic wastewater containing toxic substances and decrease the caloric value of sludge. To address this challenge, a hydrate-based method was proposed as a solution for both sludge dewatering and simultaneous discharges of clean water. Our study investigates the mechanism and feasibility of gas hydrate in sludge dewatering using a visual Nuclear Magnetic Resonance system to observe the spatial and temporal distribution of liquid water during the sewage sludge dewatering process with a crystal hydrate phase change. Our findings indicate that hydrate formation drives directional water transport and transforms part of the bound water irreversibly into free water. The results reveal that the relative percentage of free water in sludge increased from 4.0% to 36.6% after hydrate dissociation, while the mechanically bound water and bound water decreased from 66.6% and 29.4% to 36.6% and 26.8%, respectively. These results demonstrate the effectiveness of the hydrate method in removing free water and improving the sludge dewatering performance. It is essential to realize the green operation of sludge dewatering while reducing energy and chemical consumption.

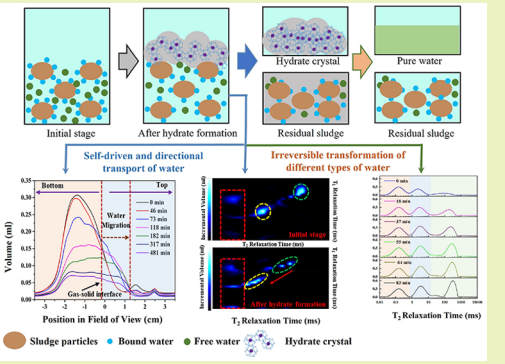

KEYWORDS: *Gas hydrate, Water migration, Irreversible transformation, Sludge conditioning, Nuclear magnetic resonance*

INTRODUCTION

The biological treatment of wastewater is crucial in reducing pollutants and protecting the environment.[1,2] However, a huge amount of sewage sludge, containing toxic substances such as pathogens, heavy metals, and organic contaminants,[3−5] remains an inevitable byproduct. The moisture content in the activated sludge exceeds 98%, and dewatering is a critical first step in further treating the sludge.[6,7]

The water present in sludge can be classified into three categories: free water, mechanically bound water (removable by mechanical strain), and bound water (not removable mechanically).[8,9] Conventional mechanical dewatering methods, such as centrifugation and filtration, are often used to remove most of the free water but are ineffective in removing the bound water.[10,11] To improve the release of interstitial or intracellular water from sludge flocs, various chemical, physical, and biological methods,[6,12,13] including Fenton oxidation,[14,15] potassium ferrate oxidation,[16] acid and alkali dissolving,[17] microwave irradiation,[18] and pyrolysis,[19,20] have been employed to disrupt the stability of highly hydrated microbial aggregations. However, these methods often result in an increase in the volume and a decrease in the calorific value of dewatered sludge due to the addition of chemical conditioning agents.[17,21] Furthermore, disrupting sludge flocs and microorganism cells can release soluble organic substances into the liquid phase, creating new high-concentration organic wastewater pollution.[22] The reduction of carbonaceous substances can further reduce the caloric value of sludge, hindering its thermal utilization as a resource for sludge incineration. In addition, the wastewater generated by the dewatering process requires additional treatment, making sludge treatment more difficult and costly.[23−26]

To increase the caloric value of dewatered sludge for improved energy recycling and simultaneously discharge clean water, a method based on clathrate hydrate was proposed for lower water content sludge dewatering. Clathrate hydrates are ice-like, nonstoichiometric crystalline compounds formed

Received: May 8, 2023
Revised: July 18, 2023
Published: August 2, 2023

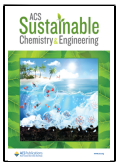

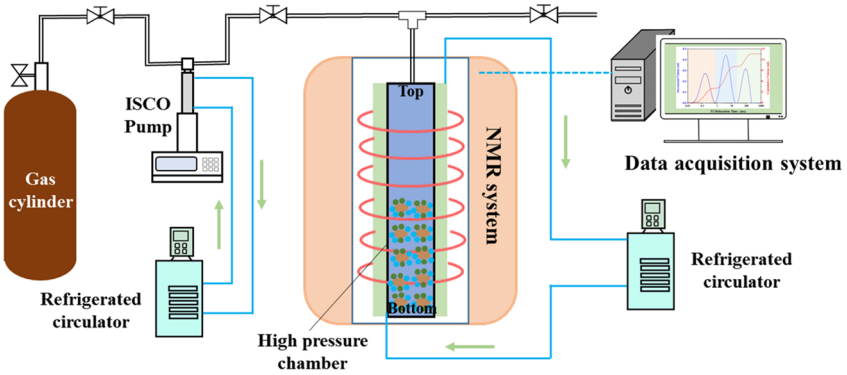

Figure 1. Schematic of an NMR experimental system.

through the encapsulation of guest molecules (such as CH_4, CO_2 and C_3H_8) in a cage-like skeleton of hydrogen-bonded water molecules, under high pressure or low temperature conditions.[27−30] During the hydrate formation, guest molecules with specific sizes can be enclathrated in a cage-like skeleton, converting liquid water into solid hydrates. Reversibly, the pure solid hydrate can be decomposed into pure water and guest molecules again via heating or depressurization.[31−35] This method has garnered attention for its applications in seawater desalination,[34] gas storage,[36−38] cold storage,[39] and sewage treatment.[40] More detailed information about hydrates can be found in Supporting Information and Figure S1. Previous research[4142] has shown that the water molecules could migrate from the bottom of the silica sand to the top of the silica sand and the hydrate was formed above the silica sand layer, which meant that hydrates exhibiting water absorption properties that can be leveraged for separation. Wu et al.[26] also observed that propane hydrate can be formed primarily on the gas−liquid interface and free water is transformed into hydrate in high-water content sludge. As we know, only liquid water molecules could be converted into solid hydrate.[27−30] High water content sludge contains a lot of liquid free water. It is easy for guest molecules to form a hydrate with liquid free water (Figure S2). However, it remains unclear whether hydrate can be formed with other types of water molecules in lower water content sludge. Besides, the transformation and migration between different types of micromoisture during the dewatering process is also unknown. Up to now, there is no relevant research on the hydrate sludge dehydration mechanism. The dehydration mechanism is essential to investigate the controlling factors and optimization of the dewatering procedure.

In this study, a visual Nuclear Magnetic Resonance (NMR) system was employed to gain a deeper understanding of the mechanism behind gas hydrate sludge dewatering. Only the ^1H in liquid water could be detected by an experimental NMR system. The presence of liquid free water will hinder the study of the dehydration mechanism. Thus, the low water content sludge was used in this study. If the bound water was transformed into free water, the transformation results could be detected by the experimental NMR system. C_3H_8 is a potential former for its moderate formation conditions.[31,41] However, the flammability and explosiveness of C_3H_8 hinder its application. Thus, the C_3H_8−CO_2 gas was used in this study. The formation and dissociation processes of gas hydrates within sludge were carefully observed, including the self-driven and directional water transport characteristics and the spatial and temporal distribution of liquid water during hydrate formation. The irreversible nature of the transformation between different types of water was also analyzed. The results of this study are critical to gaining a deeper understanding of the mechanism of sludge dewatering using gas hydrates.

MATERIALS AND METHODS

Experimental Materials and Apparatus. Sewage sludge samples were supplied by the Dalian Municipal Bureau of Ecological Environment. The sludge was obtained after high-pressure filtration, and the moisture content was about 83%. C_3H_8 (99.99%) and CO_2 (99.99%) gases were supplied by Dalian Special Gases Co., Ltd., China. C_3H_8 (16%)−CO_2 (84%) gas mixture was obtained by mixing the pure gases at 274.15 K.

The schematic of the experimental system is shown in Figure 1. A gas supply system consists of gas cylinder, pipeline and ISCO pumps with a precision of ±0.001 MPa (500 D, Teledyne ISCO Inc., U.S.A.). Two refrigerated circulators with a precision of ±0.01 K. (F38-EH, JULABO Inc., Germany) are used to control the temperature of sample chamber and gas. A low-field ^1H NMR system (12 MHz proton, GeoSpec12, Oxford, 0.3 T) is composed of the permanent magnet, a high-pressure sample chamber with an internal diameter of 25 mm and a height of 50 mm, and a data acquisition and analysis system; The double half-space SPRITE and CPMG pulse sequences were used to obtain 1D saturation at different field of view (FOV) positions and T2 relaxation times, respectively. The high-pressure sample chamber was surrounded by a cooling jacket to control the temperature, with carbon tetrafluoride used as the circulating coolant to minimize the interference of radio frequency field artifacts on the NMR detector system. The FOV of the NMR was 70 × 70 mm^2.

Experimental Procedure. The high-pressure sample chamber was positioned vertically within the NMR system during the experiment. Before experiments, half of the chamber was filled with sludge. The temperature of refrigerated circulators was set at 283.15 K. When the temperature of the high-pressure sample chamber was maintained at 283.15 K, the C_3H_8−CO_2 mixed gas was then injected from the top, maintaining a stable pressure of 2.0 MPa and temperature of 283.15 K. Subsequently, the temperature of refrigerated circulators was set at 274.15 K. Then, the temperature of the high-pressure sample chamber was decreased to 274.15 K, allowing for hydrate formation. After complete hydrate formation, the temperature was increased to 288.15 K for inducing hydrate dissociation. The pressure and gas consumption were continuously recorded with the use of Teledyne ISCO software. The NMR signals corresponding to each process were acquired separately, allowing for a clear distinction between each individual experiment. It takes 6 min and 52 s for the double half-space SPRITE and CPMG pulse sequences. The NMR signals were obtained every 2 min. The time referred to as 0 min indicates the start of the temperature decrease in the chamber. Further details can be found in our previous studies.[41]

https://doi.org/10.1021/acssuschemeng.3c02718
ACS Sustainable Chem. Eng. 2023, 11, 12075−12083

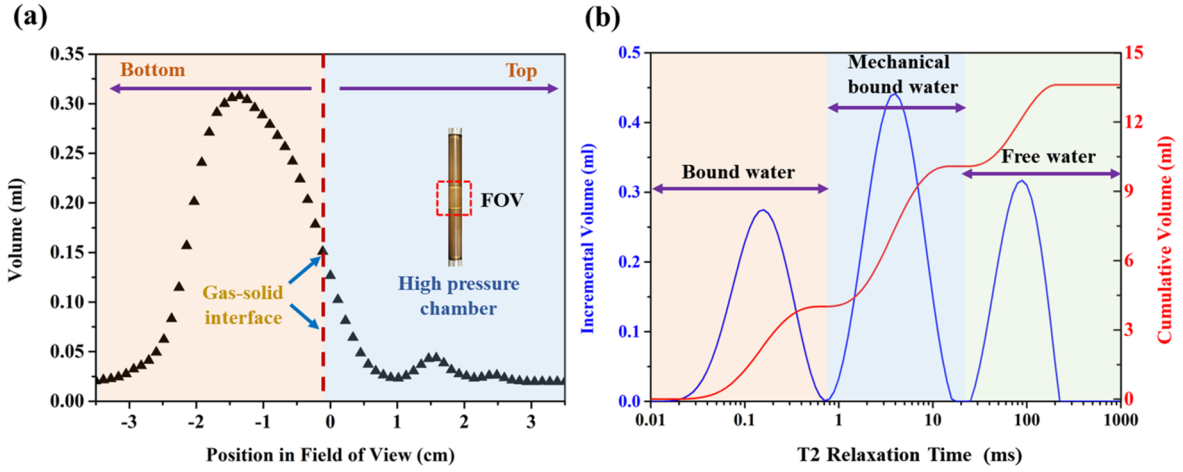

Figure 2. (a) Spatial distribution of moisture in sludge in the initial stage; (b) T2 distribution curves of sludge samples.

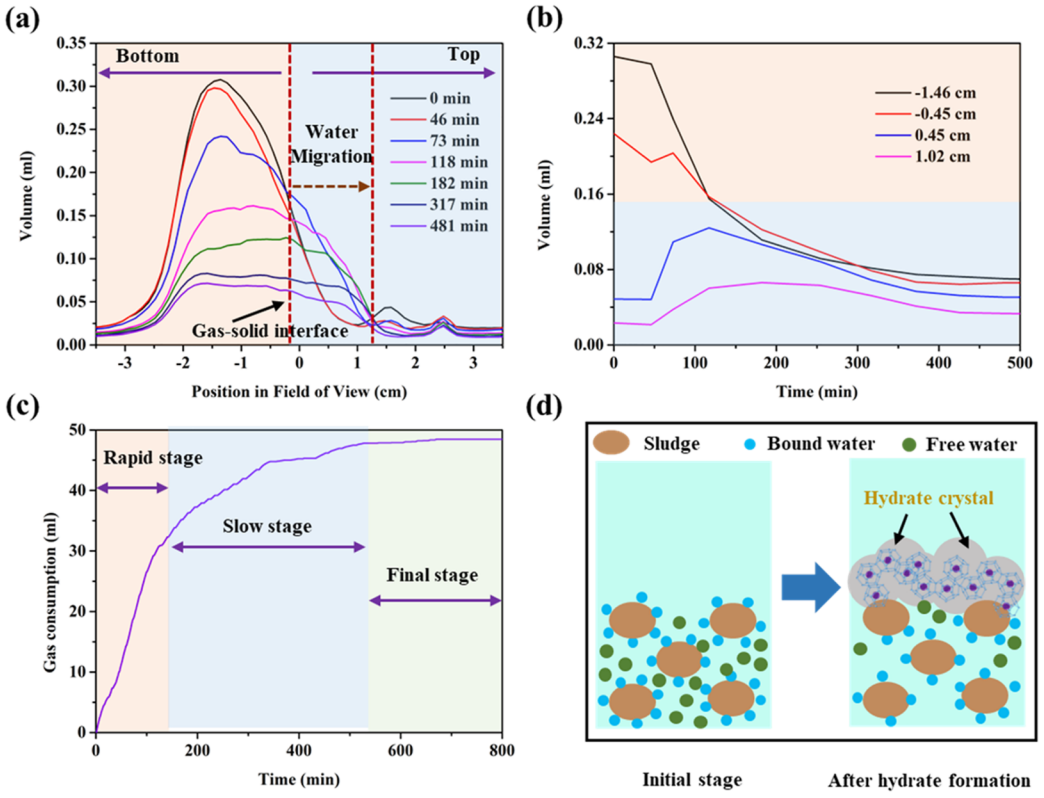

Figure 3. (a) Spatial and temporal distribution of liquid water in sludge sample during hydrate formation; (b) Change in water volume at different positions; (c) Volume of gas consumption; (d) Schematic of hydrate formation in sludge sample.

Spatial Distribution of Moisture in Sludge. After the gas injection, the position of the gas−sludge interface was determined, and the spatial distribution of water in the sludge is shown in Figure 2a,b. The FOV for the chamber corresponds to a position between −2.50 and 2.50 cm along the horizontal axis, and the 0 cm mark corresponds to the central position of the entire FOV. According to the measurement results of NMR in Figure 2a, the position of the gas−sludge interfaces is at −0.11 cm.

T_2 is the relaxation time, which could reflect the internal chemical environment of the hydrogen proton in sludge. The greater binding force of the hydrogen proton suffered or the smaller degrees of freedom of hydrogen proton, the smaller relaxation time value appears. On the contrary, free water corresponds to a larger relaxation time value. Figure 2b shows that there are three separate peaks in the T2 distribution curves at about 0.158, 3.981, and 89.125 ms, respectively. With the increase in the relaxation time, the three peaks represent bound water, mechanically bound water, and free water.

RESULTS AND DISCUSSION

Previous studies[6−9] have demonstrated that conventional mechanical dewatering is most effective in removing free water in sludge, while mechanically bound water or bound water poses a greater challenge in the dewatering process. To date, there has been no investigation into the potential of the hydrate method for removing mechanically bound water or bound water to achieve in-depth dewatering for filter-pressed sludge, and the exact mechanism behind this process remains elusive.

https://doi.org/10.1021/acssuschemeng.3c02718
ACS Sustainable Chem. Eng. 2023, 11, 12075−12083

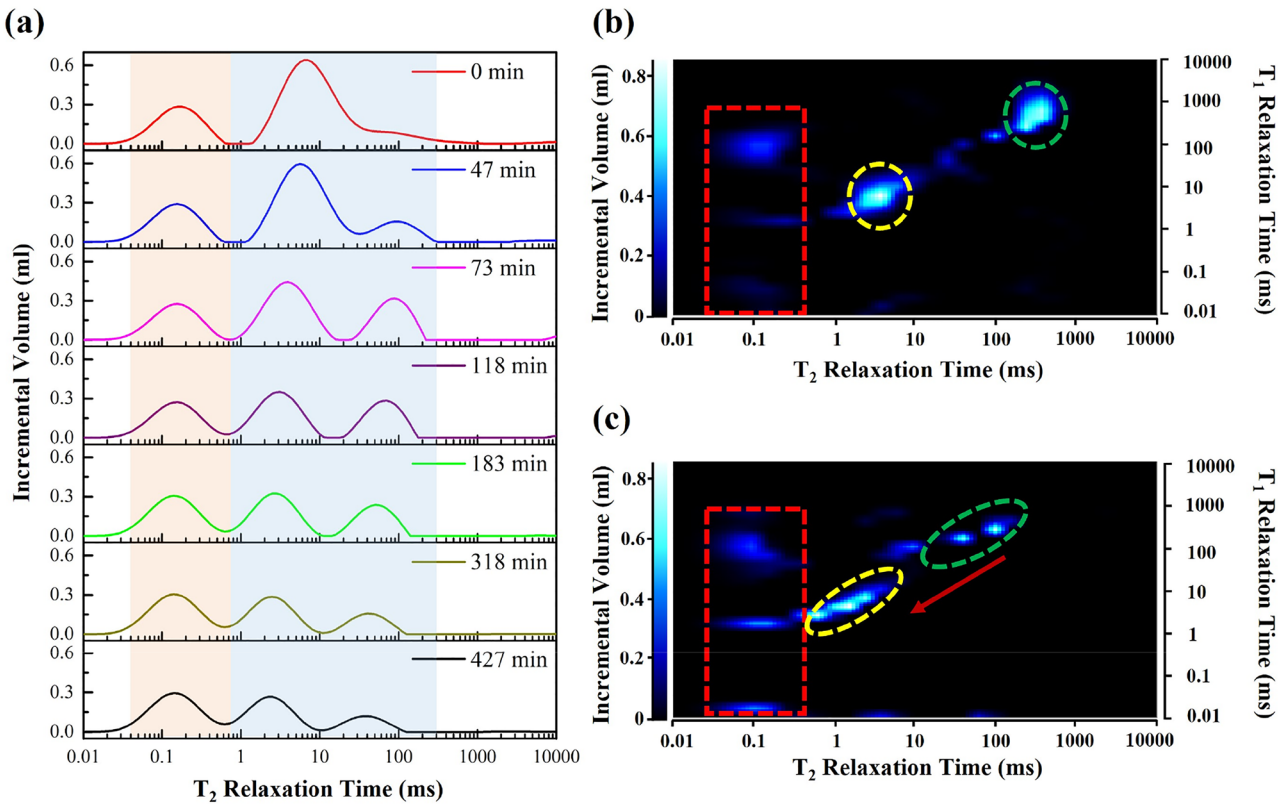

Figure 4. (a) T_2 distribution during hydrate formation; T1−T2 distributions: (b) the initial stage (0 min) and (c) the final stage (after complete hydrate formation).

Spatiotemporal Distribution and Self-Driven Directional Migration of Water in the Sludge Dewatering Process. The ^{1}D DHK SPRITE signals represent the number of free hydrogen protons and could be used to monitor the temporal and spatial variations of water in sludge. As we know, only the ^{1}H in liquid water can be detected via the NMR system. If there is water, the volume value will be greater than 0. If there is no water, the volume is 0. Similarly, if there is water between sludge particles, then the volume will have a value.

Figure 3a,b shows the spatial and temporal distributions of liquid water in sludge during the hydrate formation process. The results in Figure 3a−c clearly suggest that the spatial distribution of liquid water and the total volume of water decrease, while gas consumption increases continuously during the entire process. It meant that water molecules contained in sludge were released and converted to solid hydrate, because only liquid water could form hydrate (Figure S3). On the other hand, the position of the gas−sludge interface was initially recorded to be at −0.11 cm. However, as shown in Figure 3a, the value of the water volume between 0 and 1.20 cm increased with time. It also meant that water molecules were transferred into the top of the sludge from other position. The gas uptake in Figure 3c demonstrated that the hydrate was formed. The data in Figure 3b also proved that a significantly increase of the number of water molecules at beyond the −0.11 cm point (above the gas-sludge interface at 0.45 and 1.02 cm) corresponding to the 50 min time point, which indicated the possible migration of water molecules from the bottom to the top of the chamber; On the other hand, liquid water was converted into solid hydrate at the same time.[41,42] The self-driven and directional transport of water is beneficial for the sludge dewatering and separation of solid hydrate and residual sludge, as shown in Figure 3d. Previous studies[41−43] proposed a capillary-driven hydrate formation mechanism in porous media to clarify the water migration phenomenon (Supporting Information, Figure S4). The driving force for water migration is the capillary force between the solid hydrates or particles. The C_3H_8−CO_2 hydrate crystals tend to grow into large grains with a loose and porous structure.[41] The loose and porous structure would enhance the capillary force and promote water migration. Finally, liquid water molecules are converted to solid hydrate. The solid hydrate could be separated with sludge particles, and dry sludge could be obtained.

The T2 relaxation time, which reflects the state of hydrogen protons in sludge,[43,44] was analyzed in Figure 4a. Initially, two distinct peaks were observed in accordance with previous studies,[6−8] suggesting the presence of mechanically bound water and bound water in filter-pressed sludge. However, as hydrate formation occurred, the value of the second peak gradually decreased and a third peak emerged. The third peak showed an initial increase followed by a decrease from 0 to 427 min. This indicated a transformation of mechanically bound water into free water, followed by consumption by hydrate formation. Throughout the process, the value of the bound water remained relatively stable.

Figure 4b,c shows the T1−T2 distributions in the initial stage and final stage. The bright spot at ∼1000 ms disappeared after hydrate formation, which meant the free water was removed from sludge. The big bright spot between 1 and 10 ms became long and narrow bright bands, which also suggested some mechanically bound water in the sludge was removed. Previous literature[41,45,46] demonstrated that the crystal particle size and packing pattern of the primary nucleation of hydrates

https://doi.org/10.1021/acssuschemeng.3c02718
ACS Sustainable Chem. Eng. 2023, 11, 12075−12083

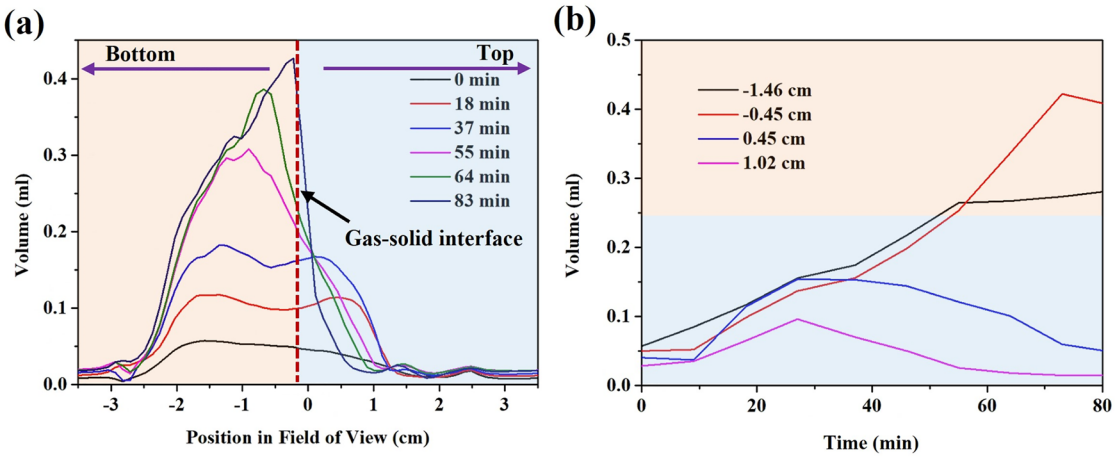

Figure 5. (a) Spatial and temporal distribution of liquid water in the sludge sample during hydrate decomposition; (b) Change in water volume at different positions.

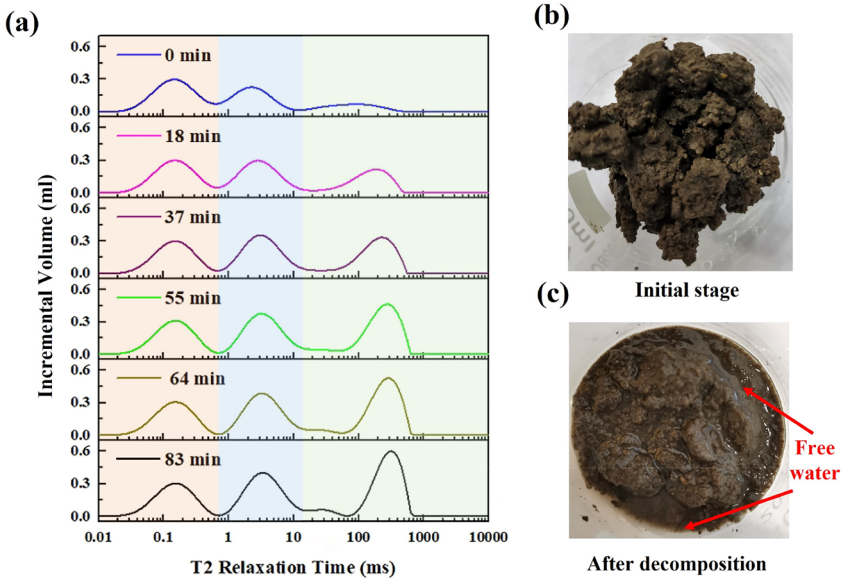

Figure 6. (a) T2 distribution during hydrate decomposition; The pictures of sludge in different stages: (b) in the initial stage before hydrate formation and (c) in the final stage after hydrate decomposition.

are essential factors that affect the transport of water molecules. The porous nature of the hydrate provides an inherently stronger capillary force to facilitate water migration. Thus, water that is physically adsorbed and mechanically captured in both micro- and macrocapillaries of capillary porous bodies[3,41] can be potentially removed. The results demonstrated that the hydrate method could be used to achieve in-depth sludge dewatering.

Reversibility Analysis of Water Transformation in Sludge Based on Hydrate Phase Change. Although hydrates can form both above the gas-sludge interface due to self-driven and directional transport of water and between sludge particles,[41,42] it is unclear whether bound water in sludge could be transformed into free water to form hydrate. It is essential to investigate the mechanism of transformation between different types of water for sewage sludge deep dewatering by the hydrate method. It is also unknown whether the crystal hydrate method has the function of sludge conditioning to improve the physicochemical and biochemical properties of sludge.

After hydrate formation, the crystal hydrates above the sludge and residual sludge could be separated easily. The crystal hydrate could be decomposed into recyclable water and gas. However, after hydrate between sludge particles dissociation, solid hydrate reverts back into free water and gas. It remains to be seen whether this decomposed free water will be reconverted to bound water.

Thus, to further analyze the mechanism of hydrate sludge dewatering, the temperature was raised to 288.15 K after hydrate formation, causing the dissociation of hydrates. Figure 5a,b displays the spatial and temporal distributions of liquid water in sludge during the decomposition process. The formation of hydrates was observed to occur above the gas−sludge interface. Upon decomposition, the volume of free water rapidly increased at the top position and ultimately accumulated at the gas−liquid interface under the influence of gravity, as shown in Figure 5a. However, the free water did not flow further into the sludge. After hydrate dissociation completely, the values at −0.45 and −1.46 cm in Figure 5b were 0.40 and 0.29 mL, respectively, which were bigger than

https://doi.org/10.1021/acssuschemeng.3c02718
ACS Sustainable Chem. Eng. 2023, 11, 12075−12083

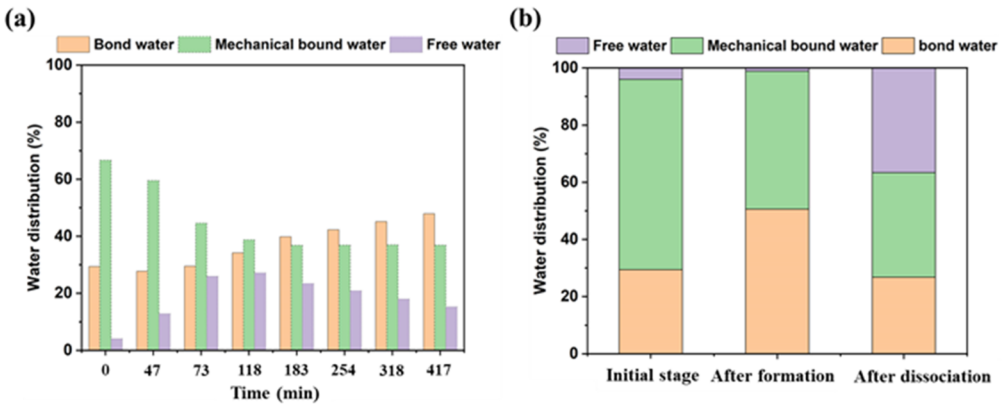

Figure 7. Variations of water distribution in sludge: (a) sewage sludge dewatering with crystal hydrate formation; and (b) comparison of relative percentage change of different types of water in different stages.

0.05 and 0.31 mL in Figure 3b. The results indicated that more free water was in sludge. In other words, some mechanically bound water was transformed into free water and these transformations were irreversible. Some of the water did not combine with the sludge again to form mechanically bound water. In the initial stage, the maximum value of water was at −1.50 cm, but after hydrate decomposition, it migrated to −0.11 cm. The migration of water also facilitated the separation of free water and sludge. It also meant that the crystal hydrate formation also had the effect of sludge conditioning. The position of hydrate formation and dissociation free water is crucial to reduce the separation difficulty and potential economic cost.

Upon hydrate formation, most of the free water was consumed and only two peaks were observed, representing mechanically bound water and bound water, respectively.[44] After hydrate formation, the temperature increased to 288.15 K for inducing hydrate dissociation. The T2 relaxation times and sludge images at various stages are presented in Figure 6a−c. The decomposition of hydrate resulted in an increase in the highest value of the second peak from 0.23 to 0.40 mL in Figure 6a. However, the corresponding value in Figure 4a was 0.64 mL, suggesting that only a portion of the decomposed free water was converted into mechanically bound water. The presence of hydrophilic substances in the sludge makes part of the free water into mechanically bound water. Meanwhile, the third peak increased significantly, with its highest value rising from 0.07 to 0.60 mL in Figure 6a. The value at 0 min in Figure 4a was 0.06 mL, indicating the appearance of new free water following hydrate formation and decomposition. A comparison of the images in the initial stage and final stage after decomposition revealed the clear presence of free water. These results demonstrate that some mechanically bound water was transformed into free water during the hydrate formation process. Although some of the free water was transformed back into mechanically bound water after hydrate decomposition, some transformations were irreversible, and the free water remained in a liquid state. This made the sludge easier to dewater.

Quantitative Analysis of the Relative Proportion of Water Transformation between Different Types of Water. Although the results demonstrate that some mechanically bound water was transformed into free water during the hydrate formation process, the relative amount of water transformation is unclear. Therefore, the relative percentage changes of different types of water moisture during the sludge dewatering process were measured and calculated. The moisture distribution in sludge was analyzed using NMR, as depicted in Figure 7a,b. The water content of each type of moisture was calculated and presented as the relative change in the water content as a percentage. At the start of the process, the relative percentages of bound water, mechanically bound water, and free water were 29.4%, 66.6%, and 4.0%, respectively (Figure 7a). During the hydrate formation process, the relative percentage of bound water increased from 29.4% to 50.6%, while the mechanically bound water decreased from 66.6% to 34.5%. The free water experienced an increase from 4.0% to 27.1% in the time period from 0 to 118 min, followed by a decrease from 27.1% to 14.9%. These results indicate that initially mechanically bound water was transformed into free water, which was then consumed by hydrate formation.

The moisture distribution in filter-pressed sludge was analyzed, as shown in Figure 7b. The results reveal a notable increase in the percentage of free water after hydrate dissociation from 4.0% in the initial stage to 36.6%. Meanwhile, the mechanical bound water and bound water decreased from 66.6% and 29.4% to 36.6% and 26.8%, respectively. This indicates that approximately 30% of the mechanically bound water was transformed into free water. It also revealed that the transformations were irreversible.

The irreversible transformations meant that the free water would not be converted into bound water again after hydrate dissociation. This property makes it easier to separate the liquid water and sludge particles, which can enhance the dewatering process. For low-water content sludge, achieving deep dewatering is difficult without the use of chemical additives. However, the use of additives can increase the total volume of solid sludge and reduce its unit caloric value, because most additives are generally noncombustible solids.

To further investigate the transformations between different types of water, the hydrate was formed in high-water and low-water content sludge, as shown in Figures S2 and S3. The high-water content sludge is liquid. The hydrate formed blocky solids in the liquid water. However, the formation finally stopped, because of the limitation of mass transfer. The pure hydrate could be obtained by solid−liquid separation. In contrast, there is little liquid water in low-water content sludge, but the self-driven water migration was observed during hydrate formation. The hydrate was formatted above the sludge. It demonstrated that some bound water was trans-

https://doi.org/10.1021/acssuschemeng.3c02718
ACS Sustainable Chem. Eng. 2023, 11, 12075−12083

formed into free water to form the hydrate. The solid hydrate was easier to separate from the sludge, and its color was whiter than that in the high-water-content sludge, indicating purer decomposed water. Only guest and water molecules can form hydrate; undesired impurities would be excluded from the hydrate crystal matrix. The application of hydrate technologies for wastewater treatment and desalination could be found in previous literature.[34,41]

Resource and energy recovery has become one of the promising goals of sludge treatment. One approach capable of achieving several treatment and recovery goals for biosolids sludge would be combustion-based technologies associated with incineration, gasification, or pyrolysis.[3] However, these combustion-based technologies require the water content below 60 wt %.[3,4] Massive chemical additives such as polymeric aluminum chloride or ferric chloride are added to the sludge to meet the water content limitation. These chemicals could reduce the calorific value of sludge, hindering its thermal utilization as a resource for sludge incineration and the chlorine introduced by commonly used chemical additives may increase the risk of dioxin formation during incineration of dewatered sludge.[47,48]

The results of this study suggest that the hydrate method can significantly enhance the sludge dewatering performance and reduce the dry solid weight while minimizing the production of high concentration organic wastewater during the dewatering process. The gases produced during hydrate decomposition can also be reused. The pure water obtained from hydrate dissociation could also discharge without further treatment. With the development of hydrate technologies, more guest molecules with mild formation conditions could be found or created, the construction cost and operation precision could be improved, and the dewaterability of sludge could be improved by reducing the pressure and increasing the temperature required for hydrate formation.[37] The advantages in secondary pollution reduction and energy savings could be beneficial for meeting the increasingly stringent environmental standards. The hydrate-based method is a potential green and sustainable technology for sludge dewatering.

CONCLUSION

In this study, the spatial and temporal characteristics of gas hydrate formation in low-water content sludge were investigated for the first time using a visual nuclear magnetic resonance system. The results revealed that hydrate formation could induce water migration from the bottom to the top of the sludge. Then the free water was converted to solid hydrate above the sludge. The self-driven and directional transport of water is beneficial for separating solid hydrates and residual sludge. The transformation of bound water to free water provided free water for water migration and hydrate formation. The loose and porous structure of the hydrate would enhance the capillary force and provide the driving force for water migration. The analysis of the water conversion efficiency suggested that approximately 30% of the mechanically bound water was transformed into free water. The results demonstrated that the transformation was irreversible. It is critical for deep sludge dewatering. After separation, the solid hydrate could be dissociated into pure water and gases again for recourse recovery. Other substances are retained in the sludge, maintaining its caloric value. The hydrate-based dewatering process provides novel insights into the sustainable development of sewage sludge dewatering.

ASSOCIATED CONTENT

Supporting Information

The Supporting Information is available free of charge at https://pubs.acs.org/doi/10.1021/acssuschemeng.3c02718.

More information and data, including the introduction of gas hydrate and the morphology of sludge and hydrate during the hydrate formation process in high-water and low-water content sludge (PDF)

AUTHOR INFORMATION

Corresponding Authors

Lunxiang Zhang − *Key Laboratory of Ocean Energy Utilization and Energy Conservation of Ministry of Education, School of Energy and Power Engineering, Dalian University of Technology, Dalian 116024, China;* orcid.org/0000-0002-3959-7575; Email: lunxiangzhang@dlut.edu.cn

Jiafei Zhao − *Key Laboratory of Ocean Energy Utilization and Energy Conservation of Ministry of Education, School of Energy and Power Engineering, Dalian University of Technology, Dalian 116024, China;* orcid.org/0000-0001-8401-4204; Email: jfzhao@dlut.edu.cn

Authors

Lingjie Sun − *Key Laboratory of Ocean Energy Utilization and Energy Conservation of Ministry of Education, School of Energy and Power Engineering, Dalian University of Technology, Dalian 116024, China; School of Geosciences, University of Edinburgh, Grant Institute, Edinburgh EH9 3FE, United Kingdom;* orcid.org/0000-0002-3301-3727

Aliakbar Hassanpouryouzband − *School of Geosciences, University of Edinburgh, Grant Institute, Edinburgh EH9 3FE, United Kingdom;* orcid.org/0000-0003-4183-336X

Huilian Sun − *Key Laboratory of Ocean Energy Utilization and Energy Conservation of Ministry of Education, School of Energy and Power Engineering, Dalian University of Technology, Dalian 116024, China*

Tian Wang − *Key Laboratory of Ocean Energy Utilization and Energy Conservation of Ministry of Education, School of Energy and Power Engineering, Dalian University of Technology, Dalian 116024, China*

Lei Yang − *Key Laboratory of Ocean Energy Utilization and Energy Conservation of Ministry of Education, School of Energy and Power Engineering, Dalian University of Technology, Dalian 116024, China;* orcid.org/0000-0003-1885-1789

Yongchen Song − *Key Laboratory of Ocean Energy Utilization and Energy Conservation of Ministry of Education, School of Energy and Power Engineering, Dalian University of Technology, Dalian 116024, China;* orcid.org/0000-0002-9752-7671

Complete contact information is available at: https://pubs.acs.org/10.1021/acssuschemeng.3c02718

Notes

The authors declare no competing financial interest.

ACKNOWLEDGMENTS

This study was supported by the National Natural Science Foundation of China (Grant Nos. 52020105007, 52025066, 52006024, and U21B2065), the National Key Research and Development Program of China (Grant No.

2022YFC2806200) and the Fundamental Research Funds for the Central Universities (Grant No. DUT22LAB130). L.S. acknowledges the support of the state scholarship fund from the China Scholarship Council (CSC202206060072).

REFERENCES

(1) Pronk, M.; de Kreuk, M. K.; de Bruin, B.; Kamminga, P.; Kleerebezem, R.; van Loosdrecht, M. C. M. Full scale performance of the aerobic granular sludge process for sewage treatment. *Water Res.* **2015**, *84* (1), 207−217.
(2) Mahmoud, A.; Olivier, J.; Vaxelaire, J.; Hoadley, A. F. *Wastewater Reuse and Management*; Springer: London, U.K., 2013.
(3) Wu, B.; Dai, X.; Chai, X. Critical review on dewatering of sewage sludge: Influential mechanism, conditioning technologies and implications to sludge re-utilizations. *Water Res.* **2020**, *180*, 115912.
(4) Hamidian, A. H.; Ozumchelouei, E. J.; Feizi, F.; Wu, C.; Zhang, Y.; Yang, M. A review on the characteristics of microplastics in wastewater treatment plants: A source for toxic chemicals. *J. Cleaner Prod.* **2021**, *295*, 126480.
(5) Huang, H.; Yuan, X. The migration and transformation behaviors of heavy metals during the hydrothermal treatment of sewage sludge. *Bioresour. Technol.* **2016**, *200*, 991−998.
(6) Zhang, W.; Xu, Y.; Dong, B.; Dai, X. Characterizing the sludge moisture distribution during anaerobic digestion process through various approaches. *Sci. Total Environ.* **2019**, *675*, 184−191.
(7) Mowla, D.; Tran, H. N.; Allen, D. G. A review of the properties of biosludge and its relevance to enhanced dewatering processes. *Bioresour. Technol.* **2013**, *58*, 365−378.
(8) Mao, H.; Wang, F.; Mao, F.; Chi, Y.; Lu, S.; Cen, K. Measurement of water content and moisture distribution in sludge by1H nuclear magnetic resonance spectroscopy. *Dry. Technol.* **2016**, *34* (3), 267−274.
(9) Vaxelaire, J.; Cezac, P. Moisture distribution in activated sludges: a review. *Water Res.* **2004**, *38* (9), 2215−2230.
(10) Cao, B.; Zhang, T.; Zhang, W.; Wang, D. Enhanced technology based for sewage sludge deep dewatering: A critical review. *Water Res.* **2021**, *189*, 116650.
(11) Li, Q.; Lu, X.; Guo, H.; Yang, Z.; Li, Y.; Zhi, S.; Zhang, K. Sewage sludge drying method combining pressurized electro-osmotic dewatering with subsequent bio-drying. *Bioresour. Technol.* **2018**, *263*, 94−102.
(12) Christensen, M. L.; Keiding, K.; Nielsen, P. H.; Jørgensen, M. K. Dewatering in biological wastewater treatment: a review. *Water Res.* **2015**, *82* (3), 14−24.
(13) Wang, Y.; Wei, Y.; Liu, J. Effect of H2O2 dosing strategy on sludge pretreatment by microwave-H2O2 advanced oxidation process. *J. Hazard. Mater.* **2009**, *169* (1), 680−684.
(14) Lin, W.; Liu, X.; Ding, A.; Ngo, H. H.; Zhang, R.; Nan, J.; Ma, J.; Li, G. Advanced oxidation processes (AOPs)-based sludge conditioning for enhanced sludge dewatering and micropollutants removal: A critical review. *J. Water Process. Eng.* **2022**, *45*, 102468.
(15) Lee, C. H.; Liu, J. C. Enhanced sludge dewatering by dual polyelectrolytes conditioning. *Water Res.* **2000**, *34* (18), 4430−4436.
(16) Ye, F.; Ji, H.; Ye, Y. Effect of potassium ferrate on disintegration of waste activated sludge (WAS). *J. Hazard. Mater.* **2012**, *219*−*220*, 164−168.
(17) Zhang, X.; Ye, P.; Wu, Y. Enhanced technology for sewage sludge advanced dewatering from an engineering practice perspective: A review. *J. Environ. Manage.* **2022**, *321*, 115938.
(18) Tyagi, V. K.; Lo, A. Microwave irradiation: A sustainable way for sludge treatment and resource recovery. *Renew. Sust. Energy Rev.* **2013**, *18*, 288−305.
(19) Barber, W. P. F. Thermal hydrolysis for sewage treatment: a critical review. *Water Res.* **2016**, *104*, 53−71.
(20) Yuan, Z.; Huang, Q.; Wang, Z.; Wang, H.; Luo, J.; Zhu, N.; Cao, X.; Lou, Z. Medium-Low Temperature Conditions Induce the Formation of Environmentally Persistent Free Radicals in Microplastics with Conjugated Aromatic-Ring Structures during Sewage Sludge Pyrolysis. *Environ. Sci. Technol.* **2022**, *56* (22), 16209−16220.
(21) Wu, B.; Chai, X.; Zhao, Y. Enhanced dewatering of waste-activated sludge by composite hydrolysis enzymes. *Bioproc. Biosyst. Eng.* **2016**, *39* (4), 627−639.
(22) Wu, B.; Wang, H.; He, Y.; Dai, X.; Chai, X. Influential mechanism of water occurrence states of waste-activated sludge: Over-focused significance of cell lysis to bound water reduction. *Water Res.* **2022**, *221*, 118737.
(23) Hu, D.; Zhou, Z.; Niu, T.; Wei, H.; Dou, W.; Jiang, L.; Lv, Y. Co-treatment of reject water from sludge dewatering and supernatant from sludge lime stabilization process for nutrient removal: A cost-effective approach. *Sep. Purif. Technol.* **2017**, *172*, 357−365.
(24) Bien, B.; Bien, J. D. Analysis of Reject Water Formed in the Mechanical Dewatering Process of Digested Sludge Conditioned by Physical and Chemical Methods. *Energies* **2022**, *15* (5), 1678.
(25) Gajewska, M.; Obarska-Pempkowiak, H. Multistage treatment wetland for treatment of reject waters from digested sludge dewatering. *Water Sci. Technol.* **2013**, *68* (6), 1223−1232.
(26) Wu, B.; Horvat, K.; Mahajan, D.; Chai, X.; Yang, D.; Dai, X. Free-conditioning dewatering of sewage sludge through in situ propane hydrate formation. *Water Res.* **2018**, *145*, 464−472.
(27) Sloan, E. D. Fundamental principles and applications of natural gas hydrates. *Nature.* **2003**, *426*, 353−359.
(28) Boswell, R.; Collett, T. S. Current perspectives on gas hydrate resources. *Energy Environ. Sci.* **2011**, *4*, 1206−1215.
(29) Sun, L.; Wang, T.; Dong, B.; Li, M.; Yang, L.; Dong, H.; Zhang, L.; Zhao, J.; Song, Y. Pressure oscillation controlled CH4/CO2 replacement in methane hydrates: CH4 recovery, CO2 storage, and their characteristics, Chem. *Eng. J.* **2021**, *425*, 129709.
(30) Zhang, L.; Sun, M.; Wang, T.; Yang, L.; Zhang, X.; Zhao, J.; Song, Y. An In-Situ MRI Method for Quantifying Temperature Changes during Crystal Hydrate Growths in Porous Medium. *J. Therm. Sci.* **2022**, *31*, 1542−1550.
(31) Hassanpouryouzband, A.; Joonaki, E.; Vasheghani Farahani, M.; Takeya, S.; Ruppel, C.; Yang, J.; English, N. J.; Schicks, J. M.; Edlmann, K.; Mehrabian, H.; Aman, Z. M.; Tohidi, B. Gas hydrates in sustainable chemistry. *Chem. Soc. Rev.* **2020**, *49*, 5225−5309.
(32) Zhang, L.; Dong, H.; Dai, S.; Kuang, Y.; Yang, L.; Wang, J.; Zhao, J.; Song, Y. Effects of depressurization on gas production and water performance from excess-gas and excess-water methane hydrate accumulations. *Chem. Eng. J.* **2022**, *431*, 133223.
(33) Zhang, L.; Ge, K.; Wang, J.; Zhao, J.; Song, Y. Pore-scale investigation of permeability evolution during hydrate formation using a pore network model based on X-ray CT, Mar. *Petrol. Geol.* **2020**, *113*, 104157.
(34) Montazeri, S. M.; Kolliopoulos, G. Hydrate based desalination for sustainable water treatment: A review. *Desalination.* **2022**, *537*, 115855.
(35) Wang, T.; Sun, L.; Fan, Z.; Wei, R.; Li, Q.; Yao, H.; Dong, H.; Zhang, L.; Yang, L.; Zhao, J.; Song, Y. Promoting CH4/CO2 replacement from hydrate with warm brine injection for synergistic energy harvest and carbon sequestration. *Chem. Eng. J.* **2023**, *457*, 141129.
(36) Zhang, L. X.; Kuang, Y. M.; Dai, S.; Wang, J. Q.; Zhao, J. F.; Song, Y. C. Kinetic enhancement of capturing and storing greenhouse gas and volatile organic compound: Micro-mechanism and micro-structure of hydrate growth. *Chem. Eng. J.* **2020**, *379*, 122357.
(37) Sun, L.; Sun, H.; Yuan, C.; Zhang, L.; Yang, L.; Ling, Z.; Zhao, J.; Song, Y. Enhanced clathrate hydrate formation at ambient temperatures (287.2 K) and near atmospheric pressure (0.1 MPa): Application to solidified natural gas technology. *Chem. Eng. J.* **2023**, *454*, 140325.
(38) Hassanpouryouzband, A.; Yang, J.; Tohidi, B.; Chuvilin, E.; Istomin, V.; Bukhanov, B. Geological CO2 Capture and Storage with Flue Gas Hydrate Formation in Frozen and Unfrozen Sediments: Method Development, Real Time-Scale Kinetic Characteristics, Efficiency, and Clathrate Structural Transition. *ACS Sustainable Chem. Eng.* **2019**, *7* (5), 5338−5345.

(39) He, T. B.; Chong, Z. R.; Zheng, J. J.; Ju, Y.; Linga, P. LNG cold energy utilization: Prospects and challenges. *Energy.* **2019**, *170*, 557−568.
(40) Sun, L.; Dong, H.; Lu, Y.; Zhang, L.; Yang, L.; Zhao, J.; Song, Y. A hydrate-based zero liquid discharge method for high-concentration organic wastewater: resource recovery and water reclamation. *NPJ Clean Water.* **2023**, *6*, 49.
(41) Sun, L.; Sun, H.; Wang, T.; Dong, H.; Zhang, L.; Yang, L.; Zhao, J.; Song, Y. Self-Driven and Directional Transport of Water During Hydrate Formation: Potential Application in Seawater Desalination and Dewatering. *Desalination* **2023**, *548*, 116299.
(42) Babu, P.; Kumar, R.; Linga, P. Unusual behavior of propane as a co-guest during hydrate formation in silica sand: Potential application to seawater desalination and carbon dioxide capture. *Chem. Eng. Sci.* **2014**, *117*, 342−351.
(43) Mao, H.; Chi, Y.; Wang, F.; Mao, F.; Liang, F.; Lu, S.; Cen, F. Effect of Ultrasonic Pre-treatment on Dewaterability and Moisture Distribution in Sewage Sludge. *Waste Biomass Valorization.* **2018**, *9*, 247−253.
(44) Rao, B.; Su, X.; Qiu, S.; Xu, P.; Lu, X.; Wu, M.; Zhang, J.; Zhang, Y.; Dong, W. Meso-mechanism of mechanical dewatering of municipal sludge based on low-field nuclear magnetic resonance. *Water Res.* **2019**, *162*, 161−169.
(45) Zhang, G.; Liu, B.; Xu, L.; Zhang, R.; He, Y.; Wang, F. How porous surfaces influence the nucleation and growth of methane hydrates. *Fuel* **2021**, *291*, 120142.
(46) Uchida, T.; Ebinuma, T.; Takeya, S.; Nagao, J.; Narita, H. Effects of Pore Sizes on Dissociation Temperatures and Pressures of Methane, Carbon Dioxide, and Propane Hydrates in Porous Media. *J. Phys. Chem. B* **2002**, *106*, 820−826.
(47) Lin, X.; Li, X.; Lu, S.; Wang, F.; Chen, T.; Yan, J. Influence of organic and inorganic flocculants on the formation of PCDD/Fs during sewage sludge incineration. *Environ. Sci. Pollut. Res.* **2015**, *22* (19), 14629−14636.
(48) Chang, S.; Lee, W.; Wang, L.; Chang-Chien, G.; Wu, C. Energy Recovery and Emissions of PBDD/Fs and PBDEs from Co-combustion of Woodchip and Wastewater Sludge in an Industrial Boiler. *Environ. Sci. Technol.* **2013**, *47* (21), 12600−12606.